Theory of electromagnetically induced waveguides

Rakesh Kapoor[1] and G. S. Agarwal[2]
[1]*Center for Advanced Technology, Indore 452 013, India*
[2]*Physical Research Laboratory, Navrangpura, Ahmedabad 380 009, Gujarat, India*
and Max Planck Institut für Quanten Optik, Garching 85748, Germany
(Received 9 August 1999; revised manuscript received 9 December 1999; published 17 April 2000)

We use a full density matrix framework and the propagation equation to study the electromagnetic field induced waveguide in an atomic vapor. We explain the experimental results of Truscott *et al.* [Phys. Rev. Lett. **82**, 1438 (1999)] for waveguiding in Rb vapor.

PACS number(s): 42.50.Gy, 42.50.Hz, 42.65.Jx, 42.65.Tg

In recent years considerable progress has been made in achieving control of the optical properties of a medium [1]. In particular the control of the dispersive properties of a medium is especially significant in several contexts. Scully and co-workers proposed enhancement of refractive index and its subsequent usage in enhancing the sensitivity of magnetometers [2]. Harris *et al.* [3] recognized the possibility of slowing the group velocity [4] of light and this has been demonstrated in recent experiments of Hau *et al.* [5] and Scully *et al.* [6]. In early works Tewari and Agarwal [7] and Harris *et al.* [8] had demonstrated the enhancement of the efficiency of VUV generation by the modifications in the absorptive and dispersive properties of a medium. These ideas have been extended to other nonlinear processes [9].

In a recent experiment Truscott *et al.* [10] demonstrated yet another important application of the modified dispersive properties of a medium. They produced an optically written waveguide in an atomic vapor. In their experiment a weak Gaussian probe beam was tuned close to the rubidium D_2 line (780 nm, $5\,^2S_{1/2}\rightarrow 5\,^2P_{3/2}$), while a strong donut shaped pump beam [11] was tuned close to the rubidium D_1 resonance (795 nm, $5\,^2S_{1/2}\rightarrow 5\,^2P_{1/2}$). The two beams interact because the two transitions share a common ground state. They used a simplified model for the susceptibilities to argue how the waveguiding can be produced.

In this paper we develop an explanation based on full density matrix equations and propagation equations in slowly varying envelop approximation. Our work includes all coherence effects. Our simulations for Doppler broadened systems produce results in excellent agreement with the work of Trusscott *et al.* Our simulations also show guiding behavior at different positions inside the cell.

We now present a theoretical model for guiding of one optical beam with another optical beam. We consider the example of the relevant energy levels of Rb. The transitions are shown in Fig. 1. We ignore the hyperfine structure of the levels for a variety of reasons [12]. The D_1 and D_2 transition of Rb can be described as a V-type atomic system. The $2\gamma's$ represent the rate of spontaneous decay. The field on the D_2 transition $|1\rangle\rightarrow|3\rangle$ is the probe field $\vec{E}_2$ while the field on D_1 transition $|2\rangle\rightarrow|3\rangle$ is the pump field $\vec{E}_1$. Δ's represent various detunings: $\Delta_1=\omega_{13}-\omega_1$ and $\Delta_2=\omega_{23}-\omega_2$, and $2G$'s denote the Rabi frequencies. $G_1=\vec{d}_{13}\cdot\vec{E}_1/\hbar, G_2=\vec{d}_{23}\cdot\vec{E}_2/\hbar$ with $\vec{d}_{\alpha\beta}$'s representing the dipole matrix elements. This type of atomic system can be described by the following set of density matrix equations

$$\dot{\rho}_{11}=-2\gamma_1\rho_{11}+iG_1\rho_{31}-iG_1^*\rho_{13}, \tag{1}$$

$$\dot{\rho}_{12}=-[\gamma_1+\gamma_2+i(\Delta_1-\Delta_2)]\rho_{12}+iG_1\rho_{32}-iG_2^*\rho_{13},$$

$$\dot{\rho}_{13}=-(\gamma_1+i\Delta_1)\rho_{13}-iG_2\rho_{12}-iG_1(\rho_{11}-\rho_{33}),$$

$$\dot{\rho}_{22}=-2\gamma_2\rho_{22}+iG_2\rho_{32}-iG_2^*\rho_{23},$$

$$\dot{\rho}_{23}=-(\gamma_2+i\Delta_2)\rho_{23}-iG_1\rho_{21}-iG_2(\rho_{22}-\rho_{33}),$$

$$\dot{\rho}_{33}=+2\gamma_1\rho_{11}+2\gamma_2\rho_{22}-iG_1\rho_{31}+iG_1^*\rho_{13}-iG_2\rho_{32}+iG_2^*\rho_{23}.$$

All the fast dependences of $\rho_{\alpha\beta}$ have been removed by canonical transformation. Thus ρ_{13} in the Schrödinger picture will be obtained by multiplying the solution of Eq. (1) by $e^{-i\omega_1 t}$. A Gaussian probe beam is tuned near to D_2 transition and a donut shaped Laguerre-Gaussian [11] pump beam of charge 3 is tuned near to D_1 transition. Thus the Rabi frequencies for pump and probe beams are given by

$$G_1=\left(\frac{G_{01}}{w_1\ (z)}\right)\sqrt{\frac{2}{\pi}}\exp\left(-\frac{ikr^2}{2q_1}\right)e^{ikz-i\omega_1 t}, \tag{2}$$

$$G_2=[G_{02}/\sqrt{3\pi}w_2\ (z)]\left(\frac{\sqrt{2}\ r}{w_2\ (z)}\right)^3 \times\exp\left(-\frac{ikr^2}{2q_2}-3i\ \theta\right)e^{ikz-i\omega_2 t}, \tag{3}$$

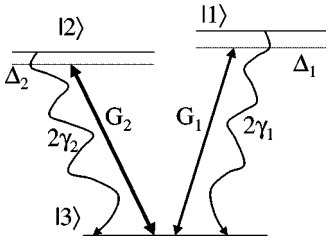

FIG. 1. A typical V system corresponding to the studies in Ref. [10].

$$r^2=x^2+y^2, \quad \theta=\tan^{-1}\left(\frac{y}{x}\right), \quad w(z)=w_{02}\sqrt{1+\left(\frac{z-z_o}{z_R}\right)^2}. \tag{4}$$

The complex parameter q in these equations can be written as $q_{1,2}=iz_{R1,2}-z+z_0$ where $z_{R1,2}=\pi w_{01,2}^2/\lambda_{1,2}$ is the Rayleigh range and the beam waist of both the beam is located at $z=z_0$. $w_{01,2}$ is the waist radius. The induced polarization for probe beam due to both the beams is taken as

$$\mathbf{P}=N\mathbf{d}_{13}\rho_{13}, \tag{5}$$

where $\mathbf{d}_{13}$ is the dipole matrix element for the D_2 transition and N is the number density. We solved the density matrix equations for steady state with the assumption of a weak probe beam and strong pump beam. Therefore in the expression for ρ_{13} the higher order terms of G_1 were neglected while keeping all orders of G_2. The value of ρ_{13} obtained with these assumption is given as

$$\rho_{13}=G_1\tilde{\chi}_{13}(\Delta_1,\Delta_2,\gamma_1,\gamma_2,|G_2|^2,\ldots). \tag{6}$$

The spatial profiles of the Rabi frequencies of the pump and probe beam leads to the spatial dependence of ρ_{13}. On scaling all the frequencies to γ_1 the expression for $\tilde{\chi}_{13}$ as obtained from the solution of Eq. (1) is given by

$$\tilde{\chi}_{13}=\frac{i(2+|G_2|^2+2\Delta_2^2)+(1+2|G_2|^2)\Delta_2+\Delta_2^3-\Delta_1(1+|G_2|^2+\Delta_2^2)}{(1+2|G_2|^2+\Delta_2^2)[2+|G_2|^2-\Delta_1^2-i\Delta_2+\Delta_1(3i+\Delta_2)]}, \quad \text{if} \quad \gamma_1=\gamma_2. \tag{7}$$

In the Rb atom the life-time of both the D_1 and D_2 transitions are more or less equal [13] therefore we have set $\gamma_2=\gamma_1$. The full susceptibility (7) differs considerably from the one used by Truscott *et al.* These differences are explained in the Appendix. This value of $\tilde{\chi}_{13}$ is valid for a cold system while for a hot system the Doppler broadening has to be taken into account [14]. The averaged $\langle\tilde{\chi}_{13}\rangle$ value in a Doppler broadened system will be given as

$$\langle\tilde{\chi}_{13}(\Delta_1,\Delta_2,\nu_D)\rangle=\int_{-\infty}^{\infty}g(\nu)\tilde{\chi}_{13}(\Delta_1-\nu,\Delta_2-\nu)d\nu, \tag{8}$$

where the weight factor $g(\nu)$ in an inhomogeneous medium is defined as

$$g(\nu)=\frac{1}{\sqrt{\pi}\nu_D}\exp[-(\nu/\nu_D)^2]. \tag{9}$$

Here ν_D is the normalized half width of the Doppler profile measured at the point where value falls to $1/e$ of maximum value. The wave equation in slowly varying envelop approximation can be written as

$$\frac{\partial G_1}{\partial z}=\frac{ic}{2\omega}\nabla_\perp^2 G_1+i\alpha\rho_{13}, \tag{10}$$

$$\nabla_\perp^2=\left(\frac{\partial^2}{\partial x^2}+\frac{\partial^2}{\partial y^2}\right),$$

where the Rabi frequency is scaled in terms of γ_1 and α is the absorption coefficient at line center

$$\alpha=\frac{4\pi n d_{13}^2\omega}{\hbar c\gamma}. \tag{11}$$

ω is the angular frequency of the transition and c is the velocity of light. In principle we should account also for the absorption and diffraction of the pump field. The equation for the pump is obtained from Eq. (10) by using the replacements $G_1\rightarrow G_2$, $\rho_{13}\rightarrow\rho_{23}$. We assume that the absorption coefficient for the two transitions are approximately equal. The density matrix element ρ_{23} can be computed to zeroth order in G_1 but to all orders in G_2.

It should be noted that the spatial transverse structure of the pump makes ρ_{13} dependent on spatial coordinate $\vec{r}$ which we have studied extensively in many different planes of the medium. Thus Eq. (10) becomes inhomogeneous. The inhomogeneities can produce Hermite-Gaussian (or Laguerre-Gauss) modes of higher order. This can be seen by expanding the inhomogeneous term in Eq. (10) in a complete set of modes. The appearance of the ring structure in the Fig. 2 is due to the excitations of modes of higher order. The experiment of Truscott *et al.* shows that there is no significant change in the pump beam while propagating through the medium. Therefore while the probe beam propagation was done numerically using the Schrödinger Eq. (10), the pump beam propagation computations were done using the analytical expression in Eq. (3). For hot system the average value of $\langle\rho_{13}\rangle$ was calculated numerically by using Eq. (7) and Eq. (8). Both the input beams are generated with an aperture large enough to pass 99% of the beam energy at its highest diameter. We consider the Rb cell of length 10 cm. First we do simulations for a hot Rb atomic vapor with Doppler broadening $\nu_D=120$. This corresponds to a Doppler width of about 690 MHz. We further take $\alpha=5100\ \text{cm}^{-1}$ corresponding to a density of about $5\times10^{12}\ \text{cm}^{-3}$. Here it was assumed that 75% ground state population was in ^{85}Rb and it was equally distributed among the two hyperfine levels of two isotopes. The pump beam was focused at the center of the cell with beam radius of 50 μm and the probe beam was focused at the entrance of the cell with beam radius of 25

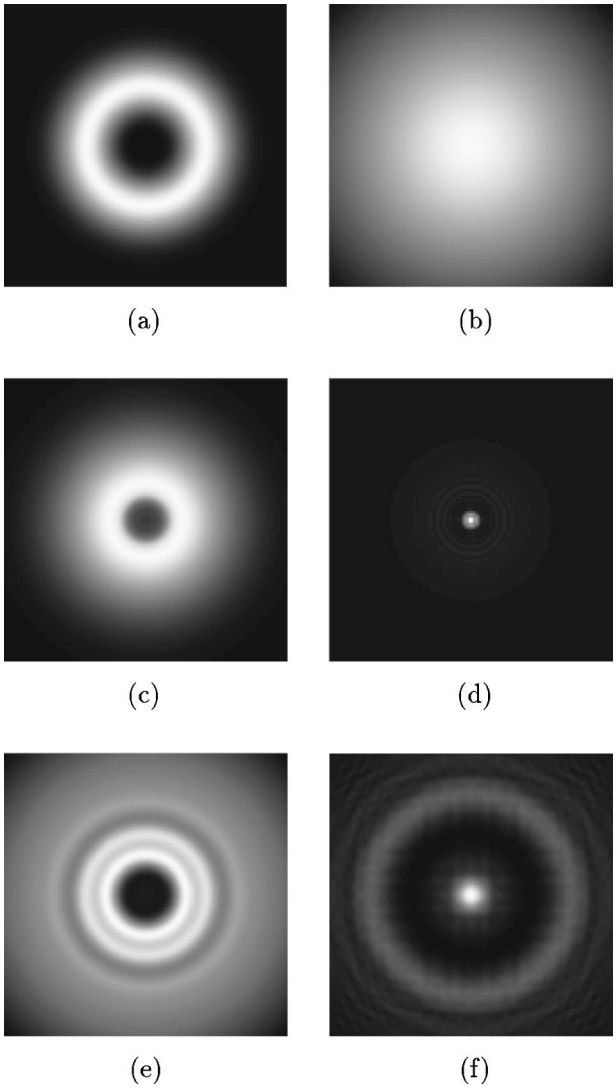

FIG. 2. The profile of the probe beam under different conditions. In the panel (a) we show the free propagating pump beam at the exit plane. The panel (b) shows the probe beam at the exit plane in the absence of pump beam but in presence of the medium with $\Delta_1/\gamma=833$. The panels (c)–(f) show probe beam profiles for different values of Δ_1 in a hot atomic system with $\nu_D/\gamma=120$ and $\Delta_2=0$,$G_{02}/\gamma=11.3$ cm and $G_{01}/\gamma=1.787$ cm. The panels (c) and (d) show recorded probe beam profile at 5 cm from the entrance window whereas panels (e) and (f) show the probe at the exit plane. In the panels (b)–(f), $\alpha=5100$ cm^{-1} and the probe beam was focused at the entrance. The probe detuning is set at $\Delta_1/\gamma=-1267$ in the panels (c), (e), and at $\Delta_1/\gamma=833$ in the panels (d) and (f).

μm. The parameter G_0 in the beam profiles has dimensions of cm/sec and is related to the power P measured in watts via the relation

$$(G_0/\gamma)\equiv\sqrt{\frac{3\lambda^3 P\times 10^7}{8\pi^2\hbar\gamma\ c}}. \tag{12}$$

For the power levels used in the experiment [10] we get $G_{02}/\gamma=11.29$ cm ($P=400$ mW), and $G_{01}/\gamma=1.78$ cm ($P=10$ mW). In all simulations a mesh size 512×512 was found to be sufficient to give accurate integral values for Eq. (7). The simulations were done for $\Delta_1=-1267$ corresponding to 3.8 GHz detuning towards blue and $\Delta_1=833$ corresponding to 2.5 GHz of detuning towards red. The pump beam was tuned to the peak of the D_1 transition, therefore $\Delta_2=0$. The probe beam profile was recorded at a plane 5 cm inside the cell and at the exit plane. The results are shown in Fig. 2. It can be seen that the redshifted probe beam gets guided into the hole of the donut while the blueshifted probe takes the shape of a ring. These results are in excellent agreement with the experimental Fig. 3 that the wave guiding occurs rather generally. This is shown by carrying out simulations for a different set of parameters.

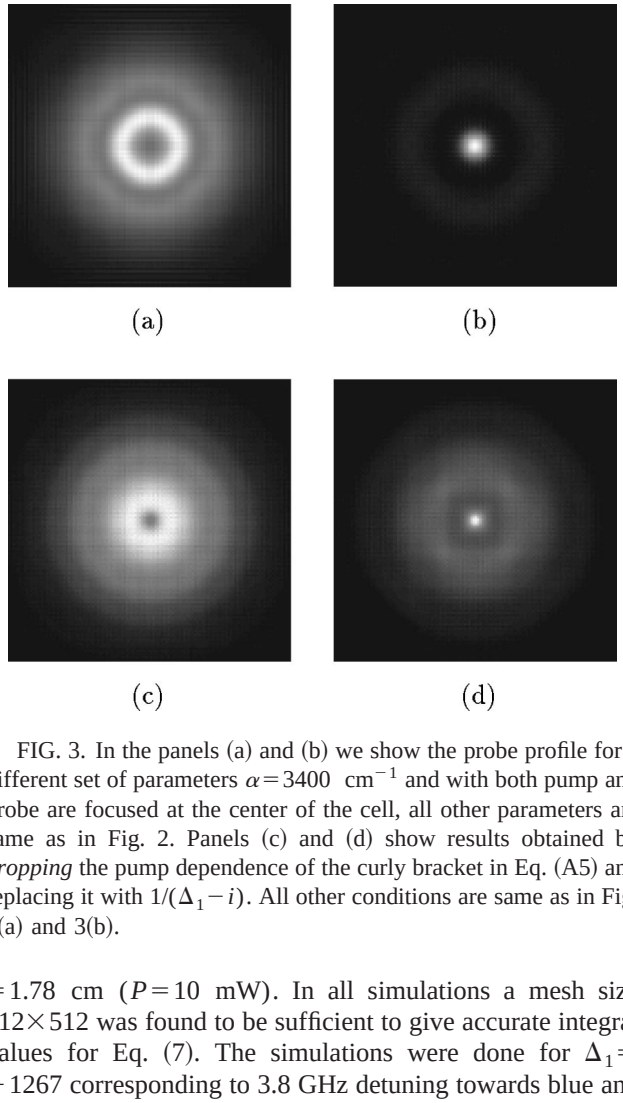

FIG. 3. In the panels (a) and (b) we show the probe profile for a different set of parameters $\alpha=3400$ cm^{-1} and with both pump and probe are focused at the center of the cell, all other parameters are same as in Fig. 2. Panels (c) and (d) show results obtained by *dropping* the pump dependence of the curly bracket in Eq. (A5) and replacing it with $1/(\Delta_1-i)$. All other conditions are same as in Fig. 3(a) and 3(b).

In conclusion we have used a general approach based on complete set of density matrix equations to study the electromagnetic field induced waveguide in vapors. All coherences are included in our work. The wave equation is solved numerically. We have explained the observations of Truscott *et al.* [10].

APPENDIX: COMPARISON OF THE SUSCEPTIBILITY (7) WITH THAT OF TRUSCOTT *et al.*

We have used the susceptibility as obtained from the complete density matrix equations for a three level V system. This susceptibility includes all coherences. We also include

Doppler broadening as indicated by our Eq. (8). The susceptibility used by Truscott *et al.* is essentially a two-level susceptibility except for the pump induced modification of the ground state population. Their Eq. (1) in our units is

$$\chi' = -\frac{2\pi N_1 d_{13}^2}{\hbar} \quad \frac{\Delta_1}{(\Delta_1^2+\Gamma_{\rm eff}^2)}, \tag{A1}$$

where $\Gamma_{\rm eff}$ is the effective line width of the $|1\rangle \leftrightarrow |3\rangle$ transition. In our notation it will be $(\gamma_1+\gamma_2)$. In Eq. (A1), N_1 is the population of the ground level. In the absence of the pump field N_1 will be equal to the total number of atoms. Truscott *et al.* argue that the pump acting on the transition $|2\rangle \leftrightarrow |3\rangle$ modifies the population of the ground state so that

$$N_1 = N\left(1+\frac{I}{2I_{\rm sat}}\right) \Big/ \left(1+\frac{I}{I_{\rm sat}}\right). \tag{A2}$$

In our notation N_1 will be

$$N_1 = N(1+|G_2|^2)/(1+2|G_2|^2). \tag{A3}$$

Thus the susceptibility used by Truscott *et al.* is

$$\chi' = -\frac{2\pi N d_{13}^2}{\hbar} \frac{\Delta_1\left(1+\frac{I}{2I_{\rm sat}}\right)}{(\Delta_1^2+\Gamma_{\rm eff}^2)\left(1+\frac{I}{I_{\rm sat}}\right)}. \tag{A4}$$

The argument used in deriving Eq. (A4) should be kept in mind. This susceptibility (A4) differs from the susceptibility obtained from the full density matrix treatment (see Ref. [14]). It may be noted that the simple argument of Truscott *et al.* misses the well-known Autler-Townes splitting. In order to see the differences, let us write Eq. (7) in the limit $\Delta_2 \to 0$

$$\tilde{\chi}_{13} = \left[\frac{1+|G_2|^2}{1+2|G_2|^2}\right] \left\{ \frac{i\left(\frac{2+|G_2|^2}{1+|G_2|^2}\right) - \Delta_1}{(2+|G_2|^2-\Delta_1^2+3i\Delta_1)} \right\}. \tag{A5}$$

Note that the full density matrix treatment leads to (a) a term [square bracket in Eq. (A5)] which is the pump induced modification of ground state population which is included in the work of Truscott *et al.*, (b) a modification of the resonant structure [curly bracket in Eq. (A5)], which is *missing* from the work of Truscott *et al.* The result of Truscott *et al.* is recovered by *dropping* the pump dependence of the curly bracket in Eq. (A5). Using the susceptibility (A5) with curly bracket replaced by $(\Delta_1 - i)^{-1}$ we show in Fig. 3 the results of numerical simulations for the same set of parameters as in Figs. 3(a) and 3(b). We include Doppler broadening. A comparison between Figs. 3(a), 3(b) and 3(c), 3(d) shows that the details (e.g., spot sizes) of the output field are different though the structure is very similar. This can be understood by the fact that if the detuning Δ_1 is much larger than both the Rabi frequency and the Doppler width, then the curly bracket in Eq. (A5) can be approximated by $1/\Delta_1$. The differences between Figs. 3(a), 3(b) and 3(c), 3(d) arise as Δ_1 is roughly of the order of the maximum value of the Rabi frequency.

[1] S. E. Harris, Phys. Today **50** (7), 36 (1997).

[2] M. O. Scully, Phys. Rev. Lett. **67**, 1855 (1991); M. O. Scully and M. Fleischhauer, *ibid.* **69**, 1360 (1992); A. S. Zibrov *et al.*, *ibid.* **76**, 3935 (1996).

[3] S. E. Harris, J. E. Field, and A. Kasapi, Phys. Rev. A **46**, R29 (1992).

[4] M. Xiao, Y. Q. Li, S. Z. Jin, and J. Gea-Banacloche, Phys. Rev. Lett. **74**, 666 (1995); R. Grobe, F. T. Hioe, and J. H. Eberly, *ibid.* **73**, 3183 (1994); A. Kasapi, M. Jain, G. Y. Yin, and S. E. Harris, *ibid.* **74**, 2447 (1995).

[5] L. V. Hau, S. E. Harris, Z. Dutton, and C. H. Behroozi, Nature (London) **397**, 594 (1999).

[6] M. M. Kash, V. A. Sautenkov, A. S. Zibrov, L. Hollberg, G. R. Welch, M. D. Lukin, Yuri Rostovtsev, E. S. Fry, and Marlan O. Scully, Phys. Rev. Lett. **82**, 5229 (1999).

[7] S. P. Tewari and G. S. Agarwal, Phys. Rev. Lett. **56**, 1811 (1986); see also G. S. Agarwal and S. P. Tewari, *ibid.* **70**, 1417 (1993).

[8] S. E. Harris, J. E. Field, and A. Imamoğlu, Phys. Rev. Lett. **64**, 1107 (1990); M. Jain, G. Y. Lin, J. E. Field, and S. E. Harris, Opt. Lett. **18**, 998 (1993).

[9] H. Schmidt and A. Imamoğlu, Opt. Lett. **21**, 1936 (1996); G. S. Agarwal and W. Harshawardhan, Phys. Rev. Lett. **77**, 1039 (1996).

[10] A. G. Truscott, M. E. J. Friese, N. R. Heckenberg, and H. Rubinsztein-Dunlop, Phys. Rev. Lett. **82**, 1438 (1999).

[11] For properties and production of Laugerre Gauss modes see L. Allen, M. W. Beijerbergen, R. J. C. Spreeuw, and J. P. Woerdman, Phys. Rev. A **45**, 8185 (1992); H. He, N. R. Heckenberg, and H. Rubinsztein-Dunlop, J. Mod. Opt. **42**, 217 (1995).

[12] We note that the sample in the experiment of Ref. [10] consists of both the isotopes ^{85}Rb and ^{87}Rb. One could, in principle, do a calculation taking the hyperfine structure into account if (i) the sample were isotopically pure, (ii) the pump and probe lasers were well stabilized, and (iii) the polarizations were well chosen, so that we know the participating magnetic sublevels. In this context it might be worth mentioning the work of H-Xia, S. J. Sharpe, A. J. Merriam, and S. E. Harris [Phys. Rev. A **56**, R3362 (1997)]. These authors examine the question of EIT with hyperfine structure in a sample of ^{207}Pb with well-polarized and well-stabilized pump and probe fields.

[13] J. Marek and P. Munster, J. Phys. B **13**, 1731 (1980).

[14] We note that EIT and gain in *V* systems have been extensively studied using (a) atomic beams [G. R. Welch, G. G. Padmabandu, E. S. Fry, M. D. Lukin, D. E. Nikonov, F. Sander, M. O. Scully, A. Weis, and F. K. Tittel, Found. Phys. **28**, 621 (1998)]; (b) cold atoms [J. Kitching and L. Hollberg, Phys. Rev. A **59**, 4685 (1999); S. A. Hopkins, E. Usadi, H. X. Chen, and A. V. Durrant, Opt. Commun. **138**, 185 (1997)], and (c) vapor cell [D. J. Fulton, S. Shepherd, R. R. Moseley, B. D. Sinclair, and M. H. Dunn, Phys. Rev. A **52**, 2302 (1995)].